Spinodal decomposition of a crystal surface

John Stewart and Nigel Goldenfeld
Loomis Laboratory of Physics, University of Illinois at Urbana-Champaign, 1110 West Green Street, Urbana, Illinois 61801
(Received 2 June 1992)

A phenomenological equation of motion for an unstable planar crystalline interface is derived and used to describe the early stages of hill and valley formation. We calculate the critical wave number for the growth of instabilities and the scattering structure function. Predictions for the temperature dependence of the width-to-length ratio and the front propagation velocity in Si are presented. The importance of an elastic interaction on the domain formation process is demonstrated and shown to explain existing experiments. Elastic interactions are also found to modify the decay rate of perturbations of stable surfaces at arbitrarily long wavelengths.

PACS number(s): 64.75.+g, 68.35.Rh, 68.35.Bs

I. INTRODUCTION

Thirty years ago, Cabrera and Mullins observed that the thermodynamics of the thermal faceting of a crystalline surface is closely analogous to the spinodal decomposition of a binary alloy [1,2]. At that time, investigation of the time dependence of the latter process had scarcely begun, but recently this has been the subject of intense study, especially since the discovery of dynamical scaling during the late stages of growth. The purpose of this paper is to resurrect Cabrera's observation and explore the consequences for the dynamics of thermal faceting of surfaces in light of the present day understanding of spinodal decomposition. To this end, we derive the equations of motion for interfaces that are the analogs of the Cahn-Hilliard equations for binary alloys. Our analysis of the linear theory including thermal fluctuations identifies the characteristic size of the early time instabilities and gives the form of the scattering form factor. We calculate the width-to-length ratio of the initial domains and the propagation velocity into the unstable state for quasi-two-dimensional systems like vicinal Si(111). Surface stress is found to have a profound effect on the dynamics precluding the possibility of dynamical scaling.

Thermal faceting is the process in which a planar crystalline surface spontaneously breaks up into a hill and valley structure following a change in temperature. For a NaCl surface at 600 °C, only the {100} planes are stable, and all other surface orientations break up into these planes. Thus if the surface of a pure NaCl crystal is prepared to coincide with the (111) plane and allowed to anneal in equilibrium with its vapor, the initially flat surface becomes tiled with the stable orientations; that is, the surface breaks up into pyramids. The equilibrium crystal shape is the Legendre transform of the surface free energy, which implies that the various stable orientations are analogous to phases of a bulk thermodynamic system and the breakup of the surface is an analog of a phase-separation process. The NaCl surface has three stable orientations and therefore three coexisting phases, as does a ternary alloy. Two-surface phase coexistence is realized for vicinal surfaces of Si(111) near the 7×7 reconstruction transition [3,4], which produces a quasi-two-dimensional pattern and exhibits only two coexisting orientations.

Cabrera [1] showed that the excluded orientations are precisely analogous to thermodynamically unstable states within the coexistence curve of a binary alloy. The amount of each facet produced is given by a lever rule, similar to the relative proportions of the coexisting phases in a binary alloy below the consolute point. The coexisting orientations are found by a double tangent construction on the relevant free energy. All important properties of coexisting binary alloys find direct analogs in thermally faceted systems. Section II contains our principal results, the presentation of the equations of motion for an interface during thermal faceting, and the consequences for small-amplitude behavior. As in the case for spinodal decomposition, we find that there is a critical wave vector, below which the initial surface is unstable. We calculate the scattering function in the linear regime. The domain shape and propagation velocity for Si are computed. Section III adds an isotropic surface stress to the equations of motion and investigates the modifications to the linear theory. We find that surface stress significantly alters the dynamics. We conclude with a discussion of the possibility of observing dynamical scaling.

II. CRYSTALLINE SURFACE DYNAMICS

We now proceed to develop the equation of motion for the approach to equilibrium of an unstable planar crystalline interface. The analogous equation for the binary alloy system is the celebrated Cahn-Hilliard equation. Our work is closely related to that of Di Carlo, Gurtin, and Podio-Guidugli, who considered the dynamics of unstable grain boundaries [5].

A. General theory

We consider two substrate dimensions, and proceed by proposing an effective free energy that includes interfacial effects. The ensuing effective chemical potential is con-

stant in equilibrium and leads us to propose an equation of motion that is the simplest equation in the effective chemical potential that obeys the conservation laws.

The coarse-grained free energy F for an unstable crystalline surface has two components: the surface free energy and the energy to form an interface between two coexisting orientations on the surface:

$$F=\int\left[\frac{\lambda}{2}[\nabla^2 z(x,y)]^2+\beta(p,q)\right]dS\ ,$$
$$\beta(p,q)=\alpha(p,q)(1+p^2+q^2)^{1/2}\ . \tag{2.1}$$

Here λ is a coefficient related to the free energy to form a corner on the surface; $z(x,y)$ is the distance to the surface from the initially flat orientation, $p=\partial z/\partial x$, $q=\partial z/\partial y$, dS is an element of substrate area; $\alpha(p,q)$ is the free-energy density of a plane with slopes p and q in the x and y directions, respectively; and $\beta(p,q)$ is the projected free-energy density. This form anticipates the linearization of the full result about an initial flat plane coincident with the x-y plane and assumes $p^2\ll 1$ and $q^2\ll 1$. The free energy F can be expressed in terms of surface invariants by replacing the $(\nabla z)^2$ with the curvature squared [5]. This introduces complications that do not affect the linear results, and are not treated here. From F, we compute the effective chemical potential of the interface $\mu=\delta F/\delta z$ to give

$$\mu=\lambda\nabla^2\nabla^2 z(x,y)-\frac{\partial}{\partial x}\frac{\partial\beta}{\partial p}-\frac{\partial}{\partial y}\frac{\partial\beta}{\partial q}\ . \tag{2.2}$$

The $(\nabla^2 z)^2$ addition to the free energy is also used in the free energy of membranes, although it arises in a completely different manner [6].

Equations of motion are derived by assuming that the system makes local changes to equalize the chemical potential while satisfying conservation laws. There are two available modes of evolution: surface diffusion and evaporation, neglecting changes to the crystalline bulk. The rate of evaporation is proportional to the difference of the chemical potential from its equilibrium value and the surface area, giving to linear order in μ:

$$\left.\frac{\partial z}{\partial t}\right|_{\text{evaporation}}=-A(\mu-\mu_{\text{eq}})(1+p^2+q^2)^{1/2}\ , \tag{2.3}$$

where A is an evaporation rate and μ_{eq} is the equilibrium surface chemical potential, which is zero for an infinite plane. Note that μ_{eq} would not be zero for a free crystal, because the equilibrium configuration is not flat, i.e., does not have zero curvature everywhere. We now proceed to the equation of motion for surface diffusion.

Surface diffusion locally conserves the area under the interface, so $z(x,y)$ should obey a continuity equation

$$\left.\frac{\partial z}{\partial t}\right|_{\text{surface diffusion}}=-\nabla\cdot\mathbf{j}\ , \tag{2.4}$$

where $\mathbf{j}$ is a surface area current. The current $\mathbf{j}$ is produced by local gradients in the surface chemical potential. The gradients are in terms of arc length, since the distance a diffusing particle must travel is measured along the surface:

$$\mathbf{j}=-B\left[\frac{\partial\mu}{\partial s_x},\frac{\partial\mu}{\partial s_y}\right]\ , \tag{2.5}$$

where $ds_x=(1+p^2)^{1/2}$ and B is a generalized mobility, which for simplicity we take to be isotropic. Substituting into the continuity equation and including evaporation, the full equation for crystalline interface evolution is

$$\frac{\partial z}{\partial t}=\left[B\frac{\partial}{\partial x}\frac{\partial}{\partial s_x}+B\frac{\partial}{\partial y}\frac{\partial}{\partial s_y}-A(1+p^2+q^2)^{1/2}\right]\times\left[\lambda\nabla^2\nabla^2 z-\frac{\partial}{\partial x}\frac{\partial\beta}{\partial p}-\frac{\partial}{\partial y}\frac{\partial\beta}{\partial q}\right]+\eta(\mathbf{r},t)\ , \tag{2.6}$$

where we have specialized to an infinite plane with $\mu_{\text{eq}}=0$. We also include a Gaussian noise $\eta(\mathbf{r},t)$ with moments

$$\langle\eta(\mathbf{r},t)\rangle=0\ ,$$
$$\langle\eta(\mathbf{r},t)\eta(\mathbf{r}',t')\rangle=-2k_B T(B\nabla^2-A)\delta^{d'}(\mathbf{r}-\mathbf{r}')\delta(t-t')\ , \tag{2.7}$$

so as to include the effects of the thermal fluctuations that guarantee that the system eventually reaches thermal equilibrium; $d'=d-1$ is the substrate dimension [7]. This equation generalizes the result of Mullins [8] with the addition of $\lambda\nabla^2\nabla^2 z$ and the noise. Mullins derived expressions for A and B:

$$A=P_0\Omega^2/\sqrt{2\pi M}\,(k_B T)^{3/2}\ , \tag{2.8}$$

$$B=\nu D_s\Omega^2/k_B T\ , \tag{2.9}$$

where P_0 is the vapor pressure of the infinite plane, Ω is the molecular volume, M is the mass, k_B is Boltzmann's constant, T is the temperature, ν is the surface density of diffusers, and D_s is the surface diffusion constant.

The equation of motion is a nonlinear partial differential equation when the free energy is of the double-well form appropriate for phase coexistence. The early stages of the dynamics after a quench can be investigated by linearizing the equations about the initial uniform state. Let

$$z=p_0 x+q_0 y+\delta z\exp(i\mathbf{k}\cdot\mathbf{x}+\omega t)\ , \tag{2.10}$$

where p_0 and q_0 specify the initial orientation, δz is a small constant, and $\omega(\mathbf{k})$ is the growth rate. Substituting into (2.6) and keeping only terms linear in δz yields the dispersion relation:

$$\omega(\mathbf{k})=-k^2(Bk^2+A)[\lambda k^2+\beta_{pp}\cos^2(\theta)+2\beta_{pq}\cos(\theta)\sin(\theta)+\beta_{qq}\sin^2(\theta)]\ ,$$
$$\beta_{pp}=\left.\frac{\partial^2\beta}{\partial p^2}\right|_{p=p_0,q=q_0},\quad \beta_{pq}=\left.\frac{\partial^2\beta}{\partial p\,\partial q}\right|_{p=p_0,q=q_0},\quad \beta_{qq}=\left.\frac{\partial^2\beta}{\partial q^2}\right|_{p=p_0,q=q_0} \tag{2.11}$$

where $k_x=k\cos(\theta)$ and $k_y=k\sin(\theta)$. If k is sufficiently small and if $\beta_{pp}<0$ or $\beta_{qq}<0$, there will be an orientation

θ where $\omega > 0$ and the interface will be unstable. This assumes p_0^2 and q_0^2 are small compared to 1. Normally, the projection plane for β is chosen so that $p_0 = 0$ and $q_0 = 0$. The theory exhibits a critical marginally stable wave vector k_c, where $\omega(k_c) = 0$:

$$k_c^2(\theta) = -\frac{1}{\lambda}[\beta_{pp}\cos^2(\theta) + 2\beta_{pq}\cos(\theta)\sin(\theta) + \beta_{qq}\sin^2(\theta)] \ . \quad (2.12)$$

If evaporation is the dominant surface process, then $B \approx 0$, and the fastest growing wave vector, which sets the characteristic domain size, is $k_{\max}^2 = \frac{1}{2}k_c^2(\theta)$. At low equilibrium vapor pressure, surface diffusion will be the dominant mode, in which case the fastest growing wave vector is $k_{\max}^2 = \frac{2}{3}k_c^2(\theta)$. As in the Cahn-Hilliard theory, the crystalline interface equations predict that the initial flat interface is unstable, and that it will separate into domains of a characteristic size.

With the linearized equation of motion for crystalline system, the evolution of its structure function at early times can be calculated. Define the structure function for a crystalline surface by

$$S(\mathbf{r},t) = \langle z(\mathbf{r},t)z(0,t)\rangle \ , \quad (2.13)$$

where $\langle\ \rangle$ denotes an average over initial conditions and over the Gaussian noise; $\mathbf{r}$ is a vector in the substrate plane. The calculation of the Fourier transform of the structure function is straightforward [9] and gives the resulting time evolution of $S(\mathbf{k},t)$:

$$S(\mathbf{k},t) = S(\mathbf{k},0)\exp[2\omega(\mathbf{k})t] - \frac{k_B T(Bk^2 + A)}{\omega(\mathbf{k})}\{1 - \exp[2\omega(\mathbf{k})t]\} \ . \quad (2.14)$$

The above results apply for any unstable crystalline surface. There are two interesting cases.

Case I. $\beta_{pp} < 0$, $\beta_{qq} < 0$: All directions on the substrate are unstable and we expect a three-dimensional pattern to form, as seen with the (111) surface of NaCl breaking up into pyramids with {100} sides.

Case II. $\beta_{pp} < 0$, $\beta_{qq} > 0$: Wave vectors are unstable in the x direction, but stable in the y direction, which implies that only modes with wave vectors near the x axis grow and a two-dimensional pattern is produced. An initially flat surface forms a quasi-two-dimensional hill and valley pattern along what we take to be the x axis. The pattern is uniform in the y direction and therefore appears as a pattern of lines from above. This behavior is indeed observed in vicinal Si(111) [10]. Additional predictions can be extracted for this case in the form of the width-to-length ratio of the initial domain and the propagation velocity into the unstable state. Because of the two-dimensional nature of the system we were also able to produce a model of the temperature dependence of the free energy. We will continue to discuss the results of our theory in terms of Si and NaCl because of the existence of decomposition experiments on the pure systems.

B. Quasi-two-dimensional results

Now we consider the dynamics for a system in the unstable regime with $\beta_{pp} < 0$ and $\beta_{qq} > 0$. For simplicity, we take $\beta_{pq} = 0$, which selects the rotation of the x-y coordinate system to be the one coinciding with the principle curvatures of β (which will change as the substrate orientation is altered). This allows the unique separation of a maximally unstable and a maximally stable direction. The pattern of lines that forms should point in the maximally stable direction, so that condition $\beta_{pq} = 0$ selects the rotation of the domains. The theory above predicts that the region is produced with dominant wave vector $k_x = k_c$ and $k_y = 0$. In Cahn-Hilliard theory, the characteristic wave number is identified as that which maximizes $\omega(\mathbf{k})$. This contains the assumption that the population of a mode in the initial configuration $S(\mathbf{k},0)$ is fairly constant over the range of wave vectors near k_c. In the binary alloy system, $\omega(\mathbf{k})$ is isotropic and this assumption should be fairly good. In the crystalline system, the critical wavelength is a function of the direction of the critical wave vector. The growth rate $\omega(\mathbf{k})$ is maximized by $k_y = 0$ but this represents a domain of infinite extent in the y direction. The population of infinite length fluctuations should be very small compared to finite-size fluctuations. We then make the following hypotheses: *The wave vector that represents domain formation is the* $\mathbf{k}$ *with the maximum* k_y *such that* $\omega(\mathbf{k}) > 0$, *i.e., the most compact marginally unstable domain.* This condition is satisfied if $dk_{yc}/d\theta = 0$, $k_{yc} = k_c\sin(\theta)$. Using the expression for the

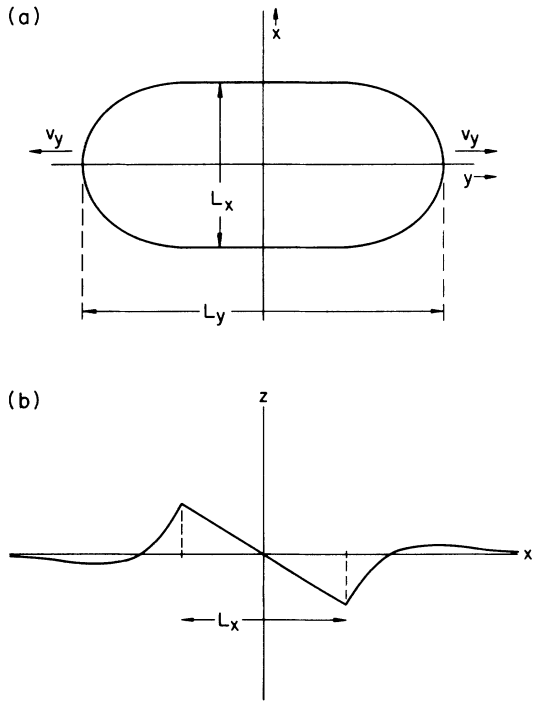

FIG. 1. Domain propagating into an unstable state. (a) Top view, (b) cross section.

critical wave vector (2.12) and setting $\beta_{pq}=0$, the characteristic wave vectors for the domain shown in Fig. 1 are

$$k_{xc}^2=\frac{-\beta_{pp}}{2\lambda}\frac{(2\beta_{qq}-\beta_{pp})}{2(\beta_{qq}-\beta_{pp})}\ , \tag{2.15}$$

$$k_{yc}^2=\frac{-\beta_{pp}}{2\lambda}\frac{(-\beta_{pp})}{2(\beta_{qq}-\beta_{pp})}\ . \tag{2.16}$$

The initial domain size L_x is given by $L_x=2\pi/k_{xc}$. This immediately gives a prediction for R:

$$R\equiv\frac{L_x}{L_y}=\left[\frac{-\beta_{pp}}{2\beta_{qq}-\beta_{pp}}\right]^{1/2}\ . \tag{2.17}$$

C. Calculation of the velocity of spreading

The final observable to be calculated is the rate at which the initial domain grows in the y direction. This is done using the marginal stability technique [11] for computing the velocity of a stable state propagating into an unstable state. The velocity is postulated to be constant and selected by the marginal stability hypothesis, as follows. Consider a perturbation moving with the front $\exp[ik_x x+ik_y y'+\phi(\mathbf{k})t]$, where $\phi(\mathbf{k})=\omega(\mathbf{k})+iv_y k_y$ is the phase and y' is measured in a frame moving with velocity v_y. The phase is required to be stationary so that the form of the front in the moving frame is maintained, and is required to be purely imaginary so that the front persists. The velocity, then, is determined by

$$\mathrm{Re}[\phi(\mathbf{k})]=0\ ,\quad \frac{\partial\phi(\mathbf{k})}{\partial k_x}=0,\frac{\partial\phi(\mathbf{k})}{\partial k_y}=0\ . \tag{2.18}$$

To simplify the calculation, we specialize to Si and assess the relative importance of surface diffusion and evaporation. The factor $A+Bk^2$ appears in the dispersion relation. The relative size of the two terms determines whether evaporation or surface diffusion dominates. The product $B\gamma$, where γ is the average isotropic surface free energy, is extrapolated from experiment [12], and is estimated to be $B\gamma=5.93\times10^{-22}$ cm^4/sec. The product $A\gamma=1.65\times10^{-16}$ cm^2/sec is calculated from (2.8) using $P_0=4.3\times10^{-8}kPa$ extrapolated from experiment $\Omega=2\times10^{-23}$ cm^3, and $\gamma=1J/m^2$ is a typical value for surface energy. For k, take $k=2\pi/L_x=0.009$ Å^{-1}, so that $B\gamma k^2=4.8\times10^{-10}$ cm^2/sec. Surface diffusion is dominant, so in computation of the velocity we set $A=0$. Inserting the dispersion relation from (2.11) into these stationary phase conditions yields

$$v_y=B\left[\frac{3}{4}\frac{-\beta_{pp}}{\lambda}\right]^{3/2}\sqrt{\beta_{qq}-\beta_{pp}}\sqrt{-\beta_{pp}}\ . \tag{2.19}$$

D. Temperature dependence

To predict the temperature dependence of k_{xc}, R, and v_y, we take the simplest form of the free energy consistent with observed phenomena and relate the parameters to the functional form of the coexistence curve as a function of temperature. The simplest surface free energy consistent with experimental observation is

$$\beta(p,q)=\gamma+\frac{\tau}{a}(p^2+q^2)^{1/2}+\frac{G}{3}[(p^2+q^2)^{1/2}]^3-\Gamma p^2\ , \tag{2.20}$$

where γ is the surface free energy of Si(111), τ is the free energy per unit length to form a ledge on the surface, G represents the entropic repulsion of adjacent ledges, and Γ is the simplest term that models the loss of convexity required for phase coexistence. The first three terms are the standard expression for the surface free energy of a vicinal surface due to Gruber and Mullins [13]. The rotationally symmetric nature of the first three terms is clearly inappropriate since they should reflect the threefold symmetry of the (111) surface. The predictions below were made setting $q_0=0$, and no q_0 dependence that is extracted from the free energy should be taken seriously. The predictions only apply to the orientations for which a coexistence curve is known. The last term is added to account for the fact that the x direction is unstable and the y direction is stable. The parameters τ, G, and Γ are related to the coexistence curve defined as $p_m(T)$, the orientation of the minority phase, by a double tangent construction that makes β convex in the x direction. For β to exhibit the observed coexistence, the following relation holds: $\Gamma(T)=2Gp_m(T)/3$. It is assumed that since Γ produces the loss of convexity that vanishes at the 7×7 transition, it carries all of the temperature dependence near the transition. Using $\Gamma(T)$ the linearized second derivatives β_{pp} and β_{qq} are computed:

$$\beta_{pp}=\tfrac{2}{3}G[3p_0-2p_m(T)]\ , \tag{2.21}$$

$$\beta_{qq}=\frac{\tau}{ap_0}+Gp_0\ , \tag{2.22}$$

where p_0 is the substrate orientation $q_0=0$. The spinodal line is defined by $\beta_{pp}=0$ and is located at orientation $p=2p_m/3$. Substitution of β_{pp} and β_{qq} into the expressions for k_{xc}, R, and v_y predicts the temperature and initial orientation dependence ($q_0=0$) of the observable parameters, providing that the coexistence curve is accurately measured. Note that we have assumed $p_0^2\ll1$, as is the case in Si, since we have not fixed $p_0=0$. For higher substrate angles, β must be transformed so that $p_0=0$.

Using the above results, crude estimates of L_x, R, and v_y are made as follows. The surface energy of the (111) plane sets the energy scale for β. We estimate $\beta_{pp}=-\gamma p^*$, where $-p^*=3p_0-2p_m$. As the temperature is raised from $T=0$, p^* approaches zero. The condition $p^*=0$ locates the spinodal line where the system turns from unstable to metastable. The corner energy can be estimated as $\lambda=a^2\gamma$, where a is the lattice spacing. Using a reasonable p^* for Si deeply in the unstable region, $p^*=0.1$, $L_x=2\pi a/(p^*)^{1/2}\approx30a$. As the spinodal is approached, $p^*\to0$ and the region size grows rapidly. It should be possible to detect the unstable region by looking for this rapid increase in domain size. Using the same estimates $R=(p^*/2)^{1/2}\approx\frac{1}{5}$, so that the domain

is elongated in the y direction. This assumes $\beta_{pp} \ll \beta_{qq}$. As $p^* \to 0$ the domain becomes increasingly elongated. Finally, $v_y \approx B\gamma p^{*2}/a^3 \approx 5 \times 10^7$ Å/sec and the growth of the region slows as the spinodal is approached.

E. Discussion of existing experiments

The physical systems of primary experimental importance are NaCl and Si.

NaCl. Knoppick and Losch [14] investigated the decomposition of NaCl(111) in equilibrium with its vapor. The equilibrium form of NaCl is a cube formed of the {100} planes until $T > 650$ °C [15]. In the decomposition experiment the (111) surface remained unstable up to the maximum experimental temperature of 800 °C, which indicates a significant impurity concentration changing the surface free energy. We will analyze the experiment as if the surface were evolving under the influence of a surface free energy that does not change over the lifetime of the experiment, i.e., neglecting impurity dynamics. There is some precedent for this: Mullin's linear facet growth theory was successfully applied to Cu covered by H_2O [16]. A (111) surface preannealed at 500 °C for 1 h is quenched to different temperatures in the unstable range and annealed for another hour. Domains in the form of pyramids with {100} sides form. The domains shrink with further annealing. While a separated surface persists until the experimental maximum temperature of 800 °C, the maximum domain size occurs at 700 °C with pyramid edge 3400 Å after 1 h, decreasing to 1400 Å after 9 h. The preannealing and evident impurity contamination make it dangerous to apply the ideas developed above to this experiment, since they assume an flat initial state and a pure system. Nevertheless, the observed behavior is consistent with our expectations when the effects of stress are included in the analysis, as shown below.

The simple theory presented above explains the breakup as resulting from $\beta_{pp} < 0$ and $\beta_{qq} < 0$ and predicts the form of the structure function, but many experimental features are inexplicable. The domain shrinkage upon annealing is completely unexpected from the binary alloy analog. The experimenters propose that the domain shrinkage results from a change of an equilibrium state resulting from the balance of the energy benefit of producing large domains against the entropy penalty as detailed by Lacmann [17]. Upon annealing, dislocations migrate and heal, and impurities segregate; this changes the free energy and therefore the equilibrium domain size. The existence of this equilibrium state is contradicted by the work of Shore *et al.* [18], who map the (111) surface onto an Ising model and find no nontrivial equilibrium state. Later we will suggest that the presence of long-range elastic forces may account for the decoarsening behavior. The temperature dependence of the initial domain size is also unexpected. The (111) plane of NaCl should represent a critical quench into the coexistence curve; as such the spinodal line should coincide with the coexistence curve. Therefore, the initial domain size should consistently shrink with temperature as predicted by (2.21). The peaking of the domain size at 700 °C is what we would expect for an off-critical quench where the spinodal line is crossed at the temperature of the peak in domain size. Simply put, in the NaCl experiment the spinodal line is not where we expect it to be.

Si. Phaneuf, Bartelt, and Williams [10] made time-resolved measurements on the order of seconds of the decomposition of vicinal surfaces of Si near the (111) plane. The surface was misoriented by 4° toward the $[\bar{2}11]$ direction and was annealed at a temperature of 848 °C, which is 3 °C below the 7×7 to 1×1 reconstruction transition temperature. An initially flat surface forms a quasi-two-dimensional hill and valley pattern along what we take to be the x axis. The pattern is uniform in the y direction and therefore appears as a pattern of lines from above. The coexistence curve has also been measured [4]. The orientation of the coexisting rough surface, which we call the minority phase, increases with decreasing temperature, Fig. 2(a). The functional dependence has a striking similarity to an alloy coexistence curve where one of the phases is constrained to be pure. The critical point for the coexistence curve is assumed to be the 7×7 reconstruction temperature T_c. At $T_c - 3$ °C the domain formation rate is slow enough that individual domain formation and propagation can be observed. The domain formation rate increases rapidly with decreasing temperature. Very near the (111) orientation the formation and extinction of nuclei is observed [19], which strongly implies the decomposition mechanism is nucleation. This contradicts the simple expression for the free energy given in (2.21) and the resultant placement of the spinodal line in Fig. 2(a). Once again the spinodal line is not where we expect it to be. The y extent of the

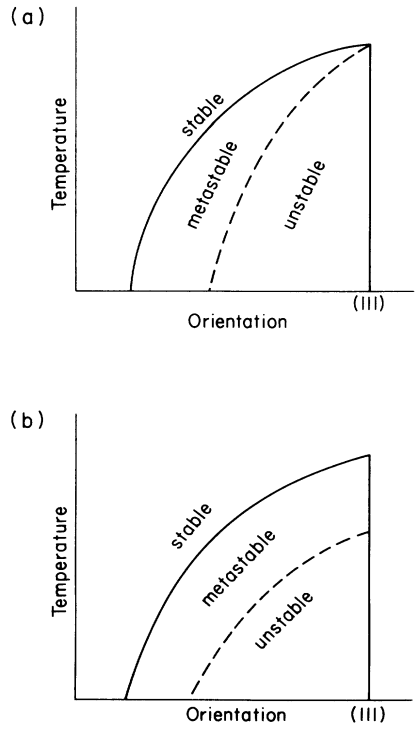

FIG. 2. Si coexistence curve (solid line) and spinodal line (dashed line). (a) Without stress, (b) with stress.

domains increases with a velocity 1000±200 Å/sec. From the estimate in the previous section, $v_y \approx B\gamma p^{*2}/a^3 \approx 5\times 10^7$ Å/sec and is therefore four orders of magnitude higher than the observed velocity, giving further evidence that the process is nucleated.

III. ELASTIC INTERACTIONS

To investigate a conjecture of Phaneuf, Bartelt, and Williams about the role of stress in the dynamics of Si, we now consider the effects of a simple isotropic elastic interaction. We have chosen such an interaction in order to simplify the analysis: a detailed theory would need to include the anisotropy of the crystal. The effect of stress in a binary-alloy system is to depress the location of the spinodal line in temperature. If the same effect were found in crystals, then the temperature dependence of the domain size in NaCl would be explained. This would also explain why nucleation behavior is seen very near the (111) orientation in Si, while (2.21) predicts an unstable mechanism. Marchencho [20] showed that under certain circumstances stress creates a nontrivial crystalline equilibrium in two-dimensional systems like Si. A nontrivial elastic equilibrium would nicely account for the deterministic decoarsening of NaCl. What follows is a continuum generalization of Marchencho's [20] work with an isotropic surface stress.

A. General results

To produce the elastic interaction term for the free energy, we first compute the elastic interaction of a set of corners on the surface. Consider an isolated corner. If we view the corner as composed of a pyramid of atoms with base lattice spacing a, then an isotropic surface stress acts along the base of the pyramid to produce a force on the corner of order ga, where g is the isotropic surface stress. The sign of the force, whether a corner is pushed up or down, depends on whether the stress is compressional or expansive. The stress force causes the bulk crystal to elastically deform until a mechanical equilibrium is reached. Since this process is spontaneous, it must result in a lowering of the free energy (the heat dissipated in the relaxation is removed by the thermal reservoir). The free-energy loss due to dissipation of kinetic energy during the relaxation is approximated by $E=-\frac{1}{2}f\delta z$, where f is the force on the corner and δz is the distance the corner travels in the deformation. If the corner is modeled as a point force on the bounding surface of an infinite isotropic elastic half space, then the displacement at a point on the interface a distance r from the force is

$$\delta z(r)=\frac{(1-\sigma^2)}{\pi Y}\frac{f}{r}\ , \tag{3.1}$$

where Y is Young's modulus and σ is Poisson's ratio for the crystalline bulk [21]. The free-energy change of an isolated corner due to stress is $E=-\frac{1}{2}f\delta z(a)$, where the singularity is cut off at a lattice spacing. Now, consider two corners a distance r apart. The distortion δz_1 at corner one is the sum of the distortions from the two forces at each corner

$$\delta z_1=\left[\frac{1-\sigma^2}{\pi Y}\right]\left[\frac{f_1}{a}+\frac{f_2}{r}\right]\ , \tag{3.2}$$

and the total elastic energy is $E=-\frac{1}{2}f_1\delta z_1-\frac{1}{2}f_2\delta z_2$. The total energy of n corners is

$$E=-\frac{1-\sigma^2}{2\pi Y}\left[\sum_i\frac{f_i^2}{a}+\sum_{i\neq j}\frac{f_if_j}{r_{ij}}\right]\ , \tag{3.3}$$

where r_{ij} is the distance between the points of application of f_i and f_j.

The next step is to develop a continuum representation of the stress relaxation of an arbitrarily curved surface in terms of a downward force per unit area. The force density is simply given by $g\nabla^2 z$, where g is the surface stress, just as if the surface were a stretched membrane. This represents a long-wavelength approximation, because we have used the Laplacian instead of the principle curvatures. The energy due to stress relaxation becomes

$$E=-\frac{C}{2}\int d\mathbf{r}\left[a(\nabla^2 z)^2+\int_{|\mathbf{r}-\mathbf{r}'|>a}d\mathbf{r}'\frac{\nabla^2 z(\mathbf{r})\nabla^2 z(\mathbf{r}')}{|\mathbf{r}-\mathbf{r}'|}\right]\ , \tag{3.4}$$

where $C=(1-\sigma^2)g^2/\pi Y$ and the a in the first term comes from converting a force density to a force. With this addition the total free energy of the surface becomes

$$F_s=\int d\mathbf{r}\left[\frac{\lambda'}{2}(\nabla^2 z)^2+\beta(p,q)-\frac{C}{2}\int_{|\mathbf{r}-\mathbf{r}'|>a}d\mathbf{r}'\frac{\nabla^2 z(\mathbf{r})\nabla^2 z(\mathbf{r}')}{|\mathbf{r}-\mathbf{r}'|}\right]\ , \tag{3.5}$$

where $\lambda'=\lambda-Ca$. Taking the functional derivative gives the chemical potential

$$\mu_s=\mu'-C\int_{|\mathbf{r}-\mathbf{r}'|>a}d\mathbf{r}'\frac{\nabla^2 z(\mathbf{r}')}{|\mathbf{r}-\mathbf{r}'|^3}\ , \tag{3.6}$$

where μ' is the chemical potential in (2.2) with the replacement $\lambda\rightarrow\lambda'$. Using the convolution theorem the dispersion relation becomes

$$\omega_s(\mathbf{k})=\omega'(\mathbf{k})-(Bk^2+A)Ck^2h(k)\ , \tag{3.7}$$

where ω' is the dispersion relation from (2.11) with the modified corner energy and $h(k)$ is the Fourier transform of $1/r^3$ with cutoff

$$h(k)=\frac{2\pi}{a}\exp(-ka)\ . \tag{3.8}$$

To zeroth order in ka, $h(k)=2\pi/a$, which gives a dispersion relation

$$\omega_s(\mathbf{k})=-(Bk^2+A)\left[\lambda' k^4+\left[\beta_{pp}+\frac{2C\pi}{a}\right]k_x^2+\left[\beta_{qq}+\frac{2C\pi}{a}\right]k_y^2\right]\ . \tag{3.9}$$

The result of adding stress is to depress the spinodal curve in temperature, as shown in Fig. 2(b). Instead of becoming unstable at $\beta_{pp}=0$ the system becomes unstable at $\beta_{pp}+2C\pi/a=0$. If we define $\beta'_{pp}=\beta_{pp}+2C\pi/a$ and $\beta'_{qq}=\beta_{qq}+2C\pi/a$ and use λ', then all the results derived without stress are valid with the substitutions $\beta_{pp}\rightarrow\beta'_{pp}$, $\beta_{qq}\rightarrow\beta'_{qq}$, and $\lambda\rightarrow\lambda'$.

Having computed the stress modified coefficients, we now evaluate the size of the effect in Si. First, an effective Young's modulus and Poisson's ratio must be estimated from the cubic elastic constants c_{11}, c_{12}, and c_{44}, by identifying c_{12} and c_{44} with the Lamé coefficients. This gives the shear modulus as $c_{44}=73.5$ GPa and the bulk compressibility as $c_{12}+2c_{44}/3=108$ GPa, yielding Young's modulus as $Y=180$ GPa$=1.125$ eV/Å^3 and Poisson's ratio as $\sigma=0.22$. The surface stress for the 7×7 plane is $g=0.185$ eV/Å^2 [22]. This gives $C=0.009$ eV/Å, $2C\pi/a=0.024$ eV/Å^2, $Ca=0.02$ eV. We have chosen the lattice spacing to be the nearest-neighbor distance in the bulk, namely 2.35 Å. It is possible that the reconstructed unit-cell size $a=47$ Å should be used, which would decrease the stress effect. To compare we take β_{pp} to be of order the surface energy estimated as $\gamma=1J/m^2=0.0625$ eV/Å^2 and we see that the stress depression of the spinodal $2C\pi/a$ is of the same order as β_{pp} and therefore is a major effect. The corner energy at $T=0$ can be estimated as $\lambda=a^2\gamma=0.3$ eV [23]. Therefore the stress contribution to the corner energy $-Ca$ is a minor effect. If $\lambda'=\lambda-Ca<0$ the system is unstable to the formation of domains at the smallest length scale of the system, which would seem to represent surface buckling. From the crude calculation above, the system is far from this transition: the surface stress would have to be increased by a factor of 3 to produce the instability.

B. Discussion of existing experiment

The nontrivial elastic equilibrium state allows the following interpretation of the NaCl experiment: Normally, the (111) plane would represent a critical quench and we would expect the spinodal (unstable) line to coincide with the coexistence curve at this point. Using the generic domain size results from Sec. II, the domain size should steadily decrease with temperature. The unexpected peak at 700 °C is explained by the stress depressing the spinodal line to this point. So in the range from 800 to 700 °C the surface is metastable and below 700 °C the surface is unstable to infinitesimal perturbations. The Marchencho equilibrium state explains the decoarsening. Below the spinodal line, the domain size is controlled by the local unstable dynamics. As the spinodal is approached the domain size diverges and it is possible that the initial domain size is larger than the elastic equilibrium size. If this were the case the initial domains would shrink under the influence of the elastic forces. This kind of elastically driven shrinking is more palatable dynamically than a force based on entropy alone. The entropy depends very weakly on domain size and so should make a weak driving force. The decoarsening in NaCl happens on a time scale consistent with normal crystalline decay experiments, suggesting an energetic driving mechanism such as elasticity.

C. Implications for decay experiments

The dispersion relation (3.7) applies equally well to the decay to equilibrium of a perturbation of a stable planar interface. Although the elastic interactions were added to account for experimental features of decomposition experiments, the calculations deriving the dispersion relation are completely general. Specifically, a surface ruled with one-dimensional sinusoidal pattern $z(\mathbf{r},0)=A_0\sin(kx)$ should evolve as $z(\mathbf{r},t)=A_0\sin(kx)\exp[\omega_s(k)t]$. Experiments that use the decay rate of sinusoidal interfaces to compute diffusion constants contain an uncontrolled systematic error due to elastic interactions. The simple computation above is insufficient to give exact quantitative information about the size of the effect but should give an order-of-magnitude estimate.

IV. DISCUSSION

Spinodal decomposition has been extensively studied because of the dynamical scaling of its structure function found in neutron-diffraction experiments. Our investigation of this system began with the hope of finding dynamical scaling. The equilibrium correspondence with the Cahn-Hilliard problem and prevalence of scaling behavior in driven surface systems [24] made scaling a very likely prospect. We however found that the simple local theory put forth in Sec. II did not explain existing experiment. The addition of a nonlocal elastic interaction qualitatively explained experiment and direct computation showed that the stress interaction could not be ignored as small. The elastic interaction generates a nontrivial equilibrium state, which precludes dynamical scaling at asymptotically long times, because the equilibrium domain size becomes a relevant length scale. The experimental equilibrium domain size is of the order of a few thousand angstroms so the coarsening process is a simple approach to equilibrium. It is possible that a crossover form may exist if systems can be found where the initial domain size is much smaller than the equilibrium domain size. This situation is found for block copolymer systems where there is also an equilibrium state characterized by a finite length scale [25]. The above analysis calls into question whether simple local interface models represent actual physical systems.

ACKNOWLEDGMENTS

We acknowledge helpful discussions with E. Williams. This work was supported in part by the National Science Foundation through Grant No. NSF-DMR-90-15791. One of us (J.S.) gratefully acknowledges the support of AT&T Bell Laboratories.

[1] N. Cabrera, *Symposium on Properties of Surfaces* (American Society for Testing and Materials, Philadelphia, 1963), p. 24.
[2] W. W. Mullins, Philos. Mag. **6**, 155 (1961).
[3] E. Williams and N. C. Bartelt, *Science* **251**, 393 (1991).
[4] E. D. Williams and N. C. Bartelt, *Ultramicroscopy* **31**, 36 (1989).
[5] A. Di Carlo, M. Gurtin, and P. Podio- Guidugli (unpublished).
[6] For a general review, see *Statistical Mechanics of Membranes and Surfaces,* edited by D. Nelson, T. Piran, and S. Weinberg (World Scientific, Singapore, 1989).
[7] H. E. Cook, Acta Metall. **18**, 297 (1970).
[8] W. W. Mullins, J. Appl. Phys. **30**, 77 (1959).
[9] J. S. Langer, M. Bar-on, and H. D. Miller, Phys. Rev. A **11**, 1417 (1975).
[10] R. J. Phaneuf, N. C. Bartelt, and E. D. Williams *et al.*, Phys. Rev. Lett. **67**, 2986 (1991).
[11] G. Dee and J. S. Langer, Phys. Rev. Lett. **50**, 383 (1983); E. Ben-Jacob, H. Brand, and L. Kramer (unpublished).
[12] W. M. Robertson, J. Am. Ceramic Soc. **64**, 9 (1981).
[13] E. E. Gruber and W. W. Mullins, J. Phys. Chem. Solids **28**, 875 (1967).
[14] D. Knoppik and A. Losch, J. Cryst. Growth **34**, 332 (1976).
[15] J. C. Heyraud and J. J. Metrois, J. Cryst. Growth **84**, 503 (1987).
[16] A. J. W. Moore, *Metal Surfaces* (American Society for Metals, Metals Park, Ohio, 1962), p. 173.
[17] R. Lacmann, in *Ergebnisse der Exacten Naturwissenschaften,* edited by G. Höhler, Springer Tracts in Modern Physics Vol. 44 (Springer-Verlag, Berlin, 1968), p. 1.
[18] J. D. Shore, J. P. Sethna, M. Holzer, and V. Elser (unpublished).
[19] E. Williams (private communication).
[20] V. I. Marchencho, Zh. Eksp. Teor. Fiz. **81**, 1141 (1981) [Sov. Phys. JETP **54**, 605 (1981)].
[21] L. Landau and L. Lifshitz, *Theory of Elasticity,* 3rd ed. (Pergamon, Oxford, 1986), p. 25.
[22] R. E. Martinez, W. M. Augustyniack, and J. Golovchenko, Phys. Rev. Lett. **64**, 1035 (1990).
[23] A. C. Shi, Ph.D. thesis, University of Illinois, 1989. The estimate is for NaCl and used as a rule of thumb for Si.
[24] M. Kardar, G. Parisi, and Y. Zhang, Phys. Rev. Lett. **56**, 889 (1986); see also H. Guo, B. Grossman, and M. Grant, *ibid.*, **64**, 1262 (1990).
[25] F. Lui and N. Goldenfeld, Phys. Rev. A **39**, 4805 (1989).